REPORT DOCUMENTATION PAGE

Form Approved
OMB No. 0704-0188

1. REPORT DATE *(DD-MM-YYYY)*	2. REPORT TYPE	3. DATES COVERED *(From - To)*
17/Jan/2002	MAJOR REPORT	

4. TITLE AND SUBTITLE
SLIDING MODE CONTROL APPLIED TO RECONFIGURABLE FLIGHT CONTOL DESIGN

5a. CONTRACT NUMBER

5b. GRANT NUMBER

5c. PROGRAM ELEMENT NUMBER

6. AUTHOR(S)
MAJ WELLS SCOTT R

5d. PROJECT NUMBER

5e. TASK NUMBER

5f. WORK UNIT NUMBER

7. PERFORMING ORGANIZATION NAME(S) AND ADDRESS(ES)
UNIVERSITY OF CALIFORNIA AT DAVIS

8. PERFORMING ORGANIZATION REPORT NUMBER
CI02-8

9. SPONSORING/MONITORING AGENCY NAME(S) AND ADDRESS(ES)
THE DEPARTMENT OF THE AIR FORCE
AFIT/CIA, BLDG 125
2950 P STREET
WPAFB OH 45433

10. SPONSOR/MONITOR'S ACRONYM(S)

11. SPONSOR/MONITOR'S REPORT NUMBER(S)

12. DISTRIBUTION/AVAILABILITY STATEMENT
Unlimited distribution
In Accordance With AFI 35-205/AFIT Sup 1

DISTRIBUTION STATEMENT A:
Approved for Public Release -
Distribution Unlimited

13. SUPPLEMENTARY NOTES

14. ABSTRACT

15. SUBJECT TERMS

16. SECURITY CLASSIFICATION OF:			17. LIMITATION OF ABSTRACT	18. NUMBER OF PAGES	19a. NAME OF RESPONSIBLE PERSON
a. REPORT	b. ABSTRACT	c. THIS PAGE		12	19b. TELEPHONE NUMBER *(Include area code)*

AIAA 2002-7751
Sliding Mode Control Applied to Reconfigurable Flight Control Design

R. A. Hess and S. R. Wells
Dept. of Mechanical and Aeronautical Engineering
University of California
Davis,

40th AIAA Aerospace Sciences Meeting & Exhibit
14 – 17 January 2002
Reno, Nevada

Sliding Mode Control Applied to Reconfigurable Flight Control Design

R.A. Hess[1] and S.R. Wells[2]
Dept. of Mechanical and Aeronautical Engineering
One Shields Ave.
University of California
Davis, CA 95616-5294

Abstract

Sliding mode control is applied to the design of flight control systems capable of operating with limited bandwidth actuators and in the presence of significant damage to the airframe and/or control effector actuators. Although inherently robust, sliding mode control algorithms have been hampered by their sensitivity to the effects of parasitic unmodeled dynamics, such as those associated with actuators and structural modes. It is known that asymptotic observers can alleviate this sensitivity while still allowing the system to exhibit significant robustness. This approach is demonstrated. The selection of the sliding manifold as well as the interpretation of the resulting linear design is accomplished in the frequency domain. The design technique is exercised on a pitch-axis controller for a simple model of the High Angle of Attack F-18 vehicle via computer simulation. A model-based tool is used for predicting task-oriented handling qualities and pilot-induced oscillation tendencies for the sliding mode controller operating with a damaged vehicle.

Introduction

Sliding Mode Control

Sliding Mode Control (SMC) is an approach to the design of control systems that exhibit robust performance in the presence of large uncertainties in plant dynamics. The basic concepts of SMC first appeared in the Russian literature in the early 1930's. In the mid 1970's sliding mode control concepts began to appear in the western literature when a text by Itkis[1] and a paper by Utkin[2] were published in English. A number of textbooks[3,4] devoted solely to SMC have since appeared as well as a vast array of papers too numerous to list. By 1993, general application areas included: robotic control, motor control, aircraft and spacecraft control, flexible structure control, and power systems.[5] Current applications also include: controlling the convergence rates for neural net learning algorithms;[6] direct robust exact differentiation;[7] missile autopilot;[8] control of multiple unmanned air vehicles in close-formation flight;[9] and reconfigurable flight control.[10]

A reconfigurable flight control system is one that is able to compensate for sudden, potentially large, unknown failure events in real-time using on-line adaptive control laws and/or adaptive redistribution of control. Of all the reconfigurable control schemes in the current literature, SMC appears to be among the most promising. This is attributable to the fact that SMC can demonstrate invariance to so-called matched uncertainty. Plant uncertainties are defined as matched when they lie in the image of the plant input matrix., i.e. the uncertainties affect the plant dynamics only through the plant input channels. Thus, if the system is invariant in the presence of uncertainties such as those arising from airframe or actuator damage, there exists no need to perform failure detection, system identification, and on-line control algorithm redesign in applying SMC to reconfigurable flight control. Indeed, it was this potential simplicity that motivated the research to be described.

Excellent review articles and surveys regarding SMC theory and applications are available, e.g. Refs. 2,5,11-15. Hence only a brief, simplified

---

[1] Professor and Vice Chairman, Associate Fellow AIAA, rahess@ucdavis.edu
[2] Graduate Student, Major, United States Air Force, Student Member AIAA

tutorial overview is given here, with emphasis on implementation and design issues.

Overview of SMC

There are several key properties of a sliding mode controller that make it very attractive for controlling an uncertain system. These properties are well known and are reviewed here without proof.[5]

- While on the sliding mode, the system dynamics are invariant to matched uncertainty.
- The hypersurface that describes $\sigma = 0$ defines the transient response of the system during the sliding mode.
- While on the sliding mode, the trajectory dynamics are of a lower order than the original model.

Consider the uncertain system with m inputs and n states given by:

$$\mathbf{x}(t) = \mathbf{A}(\mathbf{x}, t) + \mathbf{B}(\mathbf{x}, t)\,\mathbf{u}(t) + f(t, \mathbf{x}, \mathbf{u}) \qquad (1)$$

Where f represents the parameter uncertainties present in the system. The vector f is assumed to be unknown but bounded by some known function of time, system state and control vectors. In simple terms, the objective of SMC is to define

a.) m sliding surfaces or manifolds, represented in vector form as $\sigma(\mathbf{x}) = 0$, and

b.) a variable structure control given by

$$\mathbf{u}(\mathbf{x}, t) = \rho\, \mathrm{sgn}(\sigma) \qquad (2)$$

such that the system is driven to the sliding surface $\sigma = 0$ in finite time and remains upon this surface for all subsequent time. When $\sigma = 0$, a sliding mode is said to have been obtained. Equation (2) is said to describe variable structure control because the control structure is dependent upon the sign of the function σ.

This problem statement implies a two-step design process. First, the sliding manifold(s) must be designed. This can be accomplished by a wide variety of approaches ranging from arbitrarily selecting desired error dynamics to an LQR-like design utilizing the state equations in the so-called regular form[4]. A different approach utilizing frequency domain methods is offered in this work. The second step is the selection of ρ such that the sliding manifold is "attractive"—this is known as the reaching condition. One of the most common methods to prove the reaching condition is the use of Lyapunov stability criteria with $V = \boldsymbol{\sigma}^T\boldsymbol{\sigma}$ as the Lyapunov function. These proofs can become very involved, especially when parameter variations are included. Even if global analytic stability bounds can be obtained, choosing ρ analytically can be problematic. This is due to the fact that not only must bounds on f be known, but also bounds on desired values of the state vector, if model reference control is desired. Estimating the latter bound is especially difficult if there is an outer loop being closed by another agent, such as a human pilot in a flight control system.

Implementation Issues

When the system is on the sliding surface ($\sigma = 0$), the control defined by Eqn. (2) is not defined and the elements of the control vector $\mathbf{u}(\mathbf{x},t)$ will oscillate at infinite frequency. This is sometimes referred to in the literature as "chattering." Others, however, would argue that chattering occurs when noise or delays appear in the switching logic resulting in high frequency oscillations in the *state variables* as well as the elements of $\mathbf{u}(\mathbf{x},t)$. The infinite frequency switching of a pure SMC is expected and results in smooth state trajectories. Nonetheless, this infinite frequency switching in $\mathbf{u}(\mathbf{x},t)$ can not be obtained in practice, except in limited applications. One of the simplest and most common methods for eliminating the infinite frequency switching in the control signal is the use of a so-called boundary layer near the sliding manifolds. This is typically accomplished by replacing the signum function of the switching control law of Eqn. (2) with saturation elements. The slope of the linear portion of the saturation element is denoted as $(1/\varepsilon,)$ with ε being the thickness of the boundary layer. The saturation elements result in a continuous control signal, however the state trajectories are no longer constrained to the sliding manifold—only to the boundary layer near it. The price of achieving this continuous control is the loss of the invariance property. Nonetheless, considerable robustness can remain with the SMC structure when boundary layers are utilized. Strictly speaking, the resulting system should be referred to as a pseudo-sliding mode controller, since true sliding mode behavior will not be in evidence. However, for the sake of simplicity, the SMC system with boundary layer is referred to here as an SMC system.

Even when a boundary layer is used, SMC systems are vulnerable to the effects of so-called parasitic dynamics, i.e., high-frequency dynamics often neglected in control system design. In flight control applications, such neglected elements may include those associated with actuation systems and structural modes. These neglected elements can also be considered equivalent to unstructured uncertainty in the plant model. Although it has been suggested

that boundary layers alone can accommodate the effects of these neglected dynamics,[16] it has been demonstrated that finite-bandwidth actuators/sensors can cause instability within the boundary layer.[15] One of the most straightforward approaches to address this problem is the use of asymptotic observers.[15] Figure 1, adopted from Ref.15 illustrates the rationale behind the use of observers in SMC systems. As the authors indicate, the observer essentially serves as a high-frequency bypass loop in the SMC system, effectively shielding the parasitic dynamics from the high frequency activity of the controller. The observer also helps mitigate the nonlinear effects of rate and position limiting of actuators--problems which are typically catastrophic to SMC systems.

Interpretation of Linear SMC Design in the Frequency Domain

Considering a linear plant or vehicle model, the SMC system including boundary layers can be interpreted as a linear system and analyzed in the frequency domain. That is, classical loop-shaping principles can be applied to the design, both in terms of choosing appropriate sliding manifolds and in evaluating the characteristics of the final SMC configuration. Note that, if a boundary layer is employed, and the boundary layer thickness is selected such that the limits of the saturation element are never reached, the control law is essentially a high gain linear controller. For example, consider a sliding function of the form

$$\sigma = c_1 \dot{e} + c_0 e + c_{-1} \int e\,dt \qquad (3)$$

and an SMC control law (with a boundary layer)

$$u = \rho\, sat\left(\frac{\sigma}{\varepsilon}\right) \qquad (4)$$

If the saturation element always operates in the linear region, the feedback control law in the Laplace domain looks like a PID controller:

$$u(s) = \frac{\rho}{\varepsilon}\sigma = \frac{\rho}{\varepsilon}\left(c_1 s + c_0 + \frac{c_{-1}}{s}\right) e(s) \qquad (5)$$

This fact can be used to help choose both the sliding function constants (c_{-1}, c_0, and c_1) and the control law gain (ρ/ε). This interpretation of the sliding function allows the use of familiar loop shaping techniques and provides insight into the behavior of the controller. This is demonstrated in the example to follow.

SMC Design Methodology

A proposed SMC design methodology can now be offered. It is couched in terms of a SISO application, with a brief discussion of extension to MIMO applications to follow. Recalling that the objectives of SMC design are finding appropriate sliding surfaces and switching logic, the procedure to be described approaches this problem from a frequency-domain based, model-reference approach.

(1) The vehicle model is obtained, along with an estimate of the frequency beyond which parasitic dynamics (or unstructured uncertainties) are likely to come into play. This frequency is referred to as the limit frequency in this discussion.

(2) A reference model is chosen. Since piloted flight control is of interest in the present application, this reference model should be selected with an eye towards Level 1 handling qualities with no pilot-induced oscillation (PIO) tendencies. An example of accomplishing this through reference model selection is given in Ref.17 based upon a pilot model-based handling qualities and PIO prediction technique introduced in Ref.18.

(3) The desired feedback structure of the control system is determined with a square system architecture. For example, if a pitch-rate command flight control system is desired, then pitch rate (q_c) becomes the output of the reference model, and estimated pitch attitude ($\hat{q}$) is fed back to the SMC system from the observer. System error is then defined as $e(t) = q_c(t) - \hat{q}(t)$. In the SISO format a control distribution matrix is defined if more than one control effector is available. The sliding manifold, σ is chosen based upon the following principles:

a) σ is derived from a tracking error expression as

$$\sigma = e(t)^{p-1} + K_{p-2} e(t)^{p-2} + \cdots + K_0 e(t) + K_{-1} \int e(t)\,dt \qquad (6)$$

where p is the relative order of the system, i.e., the number of times the vehicle output must be differentiated for the input to appear. Note that the $(p-1)^{st}$ derivative of the error signal is included in the definition of σ. An integral term also appears in Eqn. (6) to counter the steady-state bias often created with the use of a boundary layer. Excluding the integral term, Eqn. (6) can be written in a more concise notation[16] as $\sigma = \left(\frac{d}{dt} + \lambda\right)^{p-1} e$. This approach allows an efficient and concise description of the error dynamics while in sliding mode. However, the following approach is pursued here:

b) Recognizing that a boundary layer is to be implemented, the control law is expressed as a linear transfer function as discussed earlier.

$$u(s) = \frac{\rho}{\varepsilon}\sigma$$

$$= K_\rho\left(s^{p-1} + K_{p-2}s^{p-2} + \cdots + K_0 + \frac{K_{-1}}{s}\right)e(s) \qquad (7)$$

The parameters K_i are chosen to provide desirable properties in the frequency domain. This means creating a loop transmission with broad K/s-like characteristics around crossover.[19] This will always be possible since enough derivatives are included in Eqn. (6) to create exact K/s characteristics beyond a certain frequency (at least as high as the limit frequency). Parasitic dynamics are deliberately excluded in this formulation. This step will involve obtaining an estimate of K_ρ, as this value will determine the crossover frequency of the loop transmission. This crossover frequency is selected to provide acceptable stability margins as obtained from a Bode plot of the loop transmission but using a value of K_ρ at least as large as the largest amplitude limit of any of the control effectors. The latter criterion is included to accommodate maximum trim positions of the control effectors. As opposed to typical designs involving loop shaping, very high crossover frequencies may result from this step. Indeed these frequencies may be well beyond the limit frequency. This result is of no immediate concern.

(4) Using the K_i's just determined in the definition of the sliding function, the existence of a sliding mode is verified in the inner loop using a true SMC. This step is completed without the observer, actuators, reference model or pilot model, i.e., assuming that no outer-loop is being utilized. If necessary, ρ is increased until sliding behavior is created. The initial value of $\rho = K_\rho$ obtained in step (3b) should be considered a lower limit in this process. While an analytical approach to determine ρ is certainly possible here, a more expedient route of establishing the sliding mode using a computer simulation of the system is also possible.

(5) A boundary layer is included in the controller by replacing the control law of Eqn. (2) with the control law of Eqn. (4). While maintaining a constant $\frac{\rho}{\varepsilon} = K_\rho$, increase ε until no high frequency switching is evident. Again, a simulation of the SMC system is a convenient way of finding this ε. Near-perfect tracking (with a continuous control signal) in the face of large parameter variations should be observed.

(6) Parasitic dynamics are included in the model. The SMC controller will very likely be unstable at this juncture.

(7) An asymptotic observer is created via pole-placement. The poles or eigenvalues should be chosen to lie within the frequency range bracketed by the limit frequency of step (1) and the bandwidth of the reference model of step (2). The choice of observer eigenvalues is of considerable importance in this formulation. Eigenvalues that are too large will defeat the purpose of the observer and amplify the effects of sensor noise, while eigenvalues that are too small will reduce the robustness of the SMC design.

(8) The frequency domain characteristics of the open and closed-loop SMC system with observer, boundary layer and reference model are examined to ensure that stability of the linear system is in evidence.

Analytical Handling Qualities Assessment

The goal of the research described herein involves the stability and performance robustness of flight control systems associated with damaged aircraft/actuators. With the exception of uninhabited vehicles, all these aircraft will be under piloted control. Thus, an analysis of the predicted handling qualities of damaged aircraft/actuators with the SMC systems is of considerable importance in determining the utility the proposed design methodology. Space does not allow a detailed description of the handling qualities assessment technique to be utilized here. References 17, 18 and 20 provide a description of the pilot-model based assessment tool that can be used. In essence, the pilot modeling approach can provide a prediction of the handling qualities levels and PIO susceptibility in a task-oriented framework. In the latter case, PIO "levels" are defined relative to a six-point PIO rating (PIOR) scale[18] with PIOR = 1 meaning no PIO tendencies and PIOR = 6 meaning very PIO prone. It should be emphasized that once a suitable pilot model has been chosen for the nominal or undamaged vehicle, it is not altered when pilot/vehicle performance is predicted for the damaged vehicle. The design example to be discussed next will include such an assessment.

The Design Methodology Applied to Reconfigurable Control

Vehicle, Sensor Noise and Actuator Models

The proposed design methodology is exercised next by means of a simple flight control example involving maintenance of system stability and performance robustness in the presence of airframe/actuator damage. The vehicle model chosen is identical to that utilized in Ref. 21. This choice

allows a direct comparison of the performance of the reconfigurable systems here and that provided in Ref. 21 where the compensation was obtained by classical loop shaping techniques. The adaptive gain scheme used in Ref. 21, however, is not implemented in this comparison. The vehicle model is taken from Ref. 22 and represents the simplified longitudinal dynamics of the NASA High Angle of Attack Research Vehicle (HARV). Longitudinal control is provided by a horizontal stabilator and pitch thrust vectoring. The vehicle, sensor noise and actuator models are given in Appendix A. Also included is a model of the vehicle with assumed damage of a 50% reduction in stabilator area. Note that amplitude and rate limits are included in the actuator models. An approximation of a fuselage bending mode is also included.

SMC Design

The SMC design will follow the procedure outline in the preceding discussion.

(1) The nominal aircraft model is given in Appendix A. A pitch-rate flight control system is desired. Two control effectors are available. To allow performance comparisons with the system of Ref. 21, the same control distribution matrix is employed between the single pseudo-control u(t) and the control effector variables $\delta_s(t)$ and $\delta_t(t)$. Thus,

$$\begin{Bmatrix} \delta_s \\ \delta_t \end{Bmatrix} = \begin{bmatrix} 1 \\ 1 \end{bmatrix} u(t) \qquad (8)$$

To demonstrate the ability of the SMC system to handle parasitic dynamics, the actuator dynamics and the approximated structural model are ignored in the control design. The limit frequency is selected as 20 rad/s.

(2) The reference model is chosen as

$$\frac{q_d}{q_c}(s) = \frac{100}{(s+5)(s+20)} \qquad (9)$$

where q_c is the pilot input from the cockpit control inceptor (a pitch-rate command) and q_d is the output of the reference model. This model yields acceptable task-independent handling qualities predictions using the pilot modeling technique of Ref.18.

(3) a.) The relative order of the vehicle dynamics (sans actuators) is 1, therefore the sliding manifold is given simply by

$$\sigma = e(t) + K_{-1} \int e(t)\, dt \qquad (10)$$

b.) Using loop shaping, the parameter K_{-1} is selected as: $K_{-1} = 20.0$. A preliminary value of $\rho = -30$, a value equal to the maximum amplitudes of the control effectors, yields excellent gain and phase margins, and a crossover frequency of 250 rad/s! The previous caveat regarding high crossover frequencies should be borne in mind at this juncture. The resulting loop transmission is shown in Fig. 2. Again, the only vehicle dynamics being considered are those of the rigid airframe.

(4) Employing a Simulink® simulation of the SMC system the existence of the sliding mode is verified. Figure 3 shows the inner loop pitch rate tracking performance and control signal for the pure SMC controller. Figure 4 shows the corresponding pseudo-control signal u(t). Filtered white noise was used as the q_d command signal. Still neglecting actuator dynamics, a 50% loss of stabilator and a thrust vector hard-over of $\delta_t = -3°$ occurs at 25 sec. Note the invariance to parameter changes and the near infinite frequency switching in the pseudo-control signal. True infinite-frequency switching is not possible in simulation for the same reason that it is unachievable in practice.

(5) A boundary layer is now added and a minimum value of $\varepsilon = 0.2$ is determined for the boundary layer width. Figures 5 and 6 show the same information as Figs.3 and 4, except with the boundary layer included. The tracking performance with failure is degraded slightly from that possible with near-infinite switching frequency but now a continuous pseudo-control signal is in evidence.

(6) The actuators and structural bending mode dynamics are now included. Although not shown here, the controller fails to stabilize the vehicle with these parasitic dynamics.

(7) An asymptotic observer is created assuming the availability of noisy measurements of $\alpha(t)$ and q(t). The eigenvalues of the observer are chosen as: $\lambda_{obs} = -10, -11$. These are seen to lie in the frequency range between the frequency limit and the bandwidth of the reference model.

(8) Figure 7 shows the transfer function from the output of the reference model to the pitch rate of the vehicle, computed with the observer loop closed, and now including the actuator and flexible mode dynamics. Using a -3 dB criterion, the bandwidth of this closed-loop system is 30 rad/s, well below the 250 rad/s value obtained without the observer. This reduction corroborates the qualitative explanation of the rationale behind including an observer in the SMC design (Fig. 1). With the exception of the lightly damped structural mode, the minimum damping ratio of any of the complex eigenvalues of this linear closed-loop system is 0.53.

The loop transmission L of unity feedback system that results in the same closed-loop transfer function $\left(\hat{q}/q_d\right)$ as that shown in Fig. 7 can be obtained. This is given by:

$$L = \frac{\left(\hat{q}/q_d\right)}{1-\left(\hat{q}/q_d\right)} \qquad (11)$$

Figure 8 shows the Bode plot of this transfer function where the structural mode has been omitted for clarity. Adequate gain and phase margins are in evidence. In addition, the -30 dB/dec slope of the magnitude portion of the Bode diagram around crossover corresponds exactly to the minimum value prescribed in classical loop-shaping designs.[19] Figure 9 is a comparison of the Bode diagrams of the loop transmission defined in Eqn. (11) and that obtained using the compensator of Ref. 21. Differences are clearly evident both in magnitude and phase. The robust properties of the SMC controller are obviously attributable to a large crossover frequency, e.g., the creation of a "high-gain" controller. The role of the observer in permitting this crossover frequency can be appreciated by considering the loop transmission in which it has been omitted. Figure 10 shows this loop transmission with negative stability margins clearly in evidence. Also shown is the loop transmission from Figs. 8 and 9 with observer eigenvalues λ = -10, -11 and that for the loop transmission for observer eigenvalues λ = -19, -20. Figure 11 shows the completed SMC system, including a pitch attitude loop now assumed to be closed by a human pilot.

System Performance with Failures

A pilot model for this vehicle and flight control system is created using the computer-aided design program discussed in Refs.17,18,20. A pitch-attitude loop pilot/vehicle crossover frequency of 1.5 rad/s is used. A random pitch-attitude command (θ_c) is created as white noise passed through the second order filter $1/(s+0.5)^2$. The RMS value of the resulting pitch attitude command is 11.5 deg.

The classical control system design of Ref. 21 is also implemented in Simulink® for comparison purposes. The block diagram for this system is shown in Fig. 12. The pilot model used in this simulation is identical to that utilized in Ref. 21. Sensor noise identical to that for the SMC system is used. It should be emphasized that the compensation element used in Ref. 21 was carefully designed to assure at least stability robustness in the presence of a variety of actuation system failures. No airframe failures, however, were included during the design.

Failure No. 1, Time Response

The first simulated failure assumes a 50% loss of stabilator area with a simultaneous failure of the thrust vectoring system (thrust vectoring frozen at δ_t = - 3 deg) and a 0.05 sec time delay introduced into the stabilator actuator. Figure 13 shows the pitch-attitude tracking performance of the pilot/vehicle system when the failure is introduced 25 sec into the simulation run. Figures 14 and 15 show the corresponding control surface deflections. As the figures indicate, satisfactory tracking performance is retained after failure.

The system of Ref. 21 is next subjected to Failure No. 1. As can be seen from Fig. 16, while pilot/vehicle tracking performance comparable to that of Fig. 13 is obtained prior to the failure at t = 25 sec, an oscillatory instability occurs shortly after the failure is introduced.

Failure No. 2, Time Response

The second simulated failure again assumes a 50% loss of stabilator area. After failure, the thrust vector actuator operates nominally but with a 0.05 sec time delay. After failure, the stabilator actuator operates with a 0.05 sec time delay and a reduction in its rate limits from 60 deg/s to 10 deg/s. Figure 17 shows the tracking performance of the pilot/vehicle system when the failure is introduced 25 sec into the simulation run. As the figure indicates, satisfactory tracking performance is retained after failure. Figure 18 shows the stabilator actuator rate indicating that after the failure, the stabilator actuator is in almost constant rate saturation. This performance is possible here since σ always remains within the boundary layer. Unfortunately, this condition cannot be guaranteed with SMC systems if rate or amplitude limits are reached with all effectors. Methods for explicitly handling amplitude and rate saturation require knowledge of both the actuator dynamics and their saturation characteristics, conditions not likely to be met when damage occurs.[23] The robust performance shown in Fig. 15 is attributable to the SMC system being implemented with two control effectors, one of which (the thrust vector control) did not have reduced saturation characteristics in the assumed failure.

The system of Ref. 21 is next subjected to Failure No. 2. As can be seen from Fig. 19, while pilot/vehicle tracking performance comparable to that of Fig. 17 is obtained prior to the failure at t = 25 sec, an oscillatory instability again occurs shortly after the failure is introduced.

Task-Dependent Analytical Handling Qualities Evaluation

Assume that task-oriented handling qualities levels are to be predicted for the random tracking task just described. The task performance requirements defined in terms of RMS tracking error (RMS_{err}) are described as:

Level 1: $(RMS_{err}) \leq 5$ deg

Level 2: $5 \text{ deg} < (RMS_{err}) \leq 10$ deg

Level 3: $(RMS_{err}) > 10$ deg

Predicted handling qualities (HQ) levels and PIO susceptibility can be obtained using the modeling procedure discussed in Refs.17,18,20. Using the handling qualities level and PIO levels discussed therein, task-oriented handling qualities and PIO levels can be predicted using the Structural model of the human pilot. In this pilot modeling approach, a Handling Qualities Sensitivity Function (HQSF)--defined as the magnitude of a transfer function obtained from the pilot model--is obtained. The magnitude is plotted on linear amplitude vs. frequency axes and compared with bounds delineating handling qualities Levels 1 - 3. The predicted handling qualities level is determined by the minimum level bound violated by the HQSF. A similar plot involving the power spectral density of a proprioceptive signal in the pilot model is used to delineate predicted PIO levels.

Failure No. 1, HQ and PIO

Using the random pitch-attitude command, the pilot/vehicle system is simulated for a 75 s run, with the failure in effect for the entire run. Pilot/vehicle tracking performance is 4.6 deg RMS pitch attitude error, within the Level 1 performance bounds. The required outer-loop bandwidth to achieve this performance is 1.5 rad/s. As Figs. 20 and 21 indicate, Level 1 handling qualities with no PIO tendencies are predicted.

Failure No. 2, HQ and PIO

Pilot/vehicle tracking performance is 5.4 deg RMS pitch attitude error, now just violating the Level 1 performance bounds. The required outer-loop bandwidth to achieve this performance is approximately 1.5 rad/s. As Figs. 22 and 23 indicate, handling qualities are now predicted to just violate the Level 1 boundary, but no PIO tendencies are indicated.

Extension to MIMO Designs

There are no intrinsic limitations of the proposed methodology to SISO systems. Under the assumption of a square system, where the number of reference model inputs are equal to the outputs to be feedback to the SMC system, the design of robust, decoupled controllers should be reasonably straightforward. A number of MIMO SMC designs are presented in tutorial fashion in the Ref. 4. The methodology proposed here for SISO designs would be applied independently to each of the control channels of the MIMO system. Again, frequency domain techniques could be employed to assess the quality of the resulting linear design.

Conclusions

1) A step-by-step procedure for the design of sliding mode controllers for reconfigurable flight control systems is feasible.
2) Asymptotic observers are shown to eliminate the well-documented sensitivity of sliding mode designs to parasitic dynamics.
3) The procedure
   a.) allows a number of the required design decisions to be made in the frequency domain, and
   b.) allows an interpretation of the robust properties of the SMC controller in terms of an effective, unity-feedback loop transmission. Viewed in this light, the SMC procedure serves as a means to an end, that being the creation of a loop transmission with stability and performance robustness in the presence of system failures.
4) In a computer simulation of a fighter pitch-rate flight control system including a model of the human pilot, the SMC system exhibits superior tracking performance and predicted handling qualities as compared to a classical control system design. This comparison included significant airframe and actuator damage.
5) The absence of requirements for failure detection, system identification and on-line algorithm redesign makes the SMC approach attractive from the standpoint of vehicle handling qualities.

Acknowledgement

This research was supported by a grant from NASA Langley Research Center. Dr. Barton Bacon serves as the grant technical manager.

Appendix A:
Nominal and Damaged Vehicle, and Sensor Noise Models

The nominal flight condition is a Mach number of 0.6 at an altitude of 30,000 ft.

$$\dot{\mathbf{x}}(t) = \mathbf{A}\mathbf{x}(t) + \mathbf{B}\mathbf{u}(t)$$

$$\mathbf{x}(t) = [\alpha(t)\ q(t)] \qquad \text{(A1)}$$

$$\mathbf{u}(t) = [\delta_s\ \delta_t]$$

where α is angle of attack (deg); q is pitch rate (deg/sec); δ_s is stabilator angle (deg); and δ_t is thrust vector angle (deg). For the nominal vehicle,

$$\mathbf{A} = \begin{bmatrix} -0.5088 & 0.994 \\ -1.131 & -0.2804 \end{bmatrix}$$
$$\mathbf{B} = \begin{bmatrix} -0.9277 & -0.01787 \\ -6.575 & -1.525 \end{bmatrix} \quad \text{(A2)}$$

For the damaged vehicle (50% reduction in stabilator area),

$$\mathbf{A}_{fail} = \begin{bmatrix} -0.48 & 0.997 \\ -0.4639 & -0.01787 \end{bmatrix}$$
$$\mathbf{B}_{fail} = \begin{bmatrix} -0.4639 & -0.01787 \\ -3.2875 & -1.525 \end{bmatrix} \quad \text{(A3)}$$

To approximate the effects of a flexible body-bending mode on the aircraft, the α and q outputs are passed through a second order dipole given by

$$\left(\frac{60^2}{50^2}\right)\left(\frac{s^2 + 2(0.005)(50)s + 50^2}{s^2 + 2(0.005)(60)s + 60^2}\right)$$

The actuator model for the stabilator is $30^2/(s^2 + 42.4s + 30^2)$, with amplitude limits of ±30 deg, and rate limits of ±60 deg/s. The actuator model for the thrust vectoring is $20^2/(s^2 + 24s + 20^2)$, with amplitude limits of ±30 deg, and rate limits of ±60 deg/s.

Sensor noise in the α and q sensors are modeled as white noise passed through filters $10^2/(s^2 + 20s + 10^2)$ producing RMS noise levels of 0.05 deg, and 0.05 deg/s, respectively.

References

[1]Itkis, Y., *Control Systems of Variable Structure*, Wiley, New York, NY, 1976.

[2]Utkin, V. I., "Variable Structure Systems with Sliding Mode," *IEEE Transactions on Automatic Control*, Vol. AC-22, No. 2, 1977, pp. 212-222.

[3]Utkin, V. I., *Sliding Modes in Control and Optimization*, Springer-Verlag, Berlin, Ger., 1992.

[4]Edwards, C., and Spurgeon, S. K., *Sliding Mode Control*, Taylor & Francis Ltd, Bristol, PA, 1998.

[5]Hung, J. Y., Weibing, G., and Hung, J. C., "Variable Structure Control: A Survey," *IEEE Transactions on Industrial Electronics*, Vol. 40, No. 1, 1993, pp. 2-23.

[6]Poznyak, A. S., Yu, W., and Sanchez, E. N., "Identification and Control of Unknown Chaotic Systems via Dynamic Neural Networks," *IEEE Transactions on Circuits and Systems-I:Fundamental Theory and Applications*, Vol. 46, No. 12, 1999, pp. 1491-1495.

[7]Levant, A., "Robust Exact Differentiation via Sliding Mode Technique," *Automatica*, Vol. 34, No. 3, 1998, pp. 379-384.

[8]Salamci, M. U., Özgören, M. K., and Banks, S. P., "Sliding Mode Control with Optimal Sliding Surfaces for Missile Autopilot Design," *Journal of Guidance, Control, and Dynamics*, Vol. 23, No. 4, 2000, pp. 719-727.

[9]Schumacher, C., and Singh, S. N., "Nonlinear Control of Multiple UAVs in Close-Coupled Formation Flight," AIAA-2000-4373, *Proceedings of Guidance, Navigation, and Control Conference*, AIAA, Denver, CO, 14-17 Aug 2000, pp. 1-7.

[10]Shtessel, Y. B., Buffington, J. M., and Banda, S. S., "Multiple Timescale Flight Control Using Reconfigurable Sliding Modes," *Journal of Guidance, Control, and Dynamics*, Vol. 22, No. 6, 1999, pp. 873-883.

[11]DeCarlo, R., A., Zak, S. H., and Mathews, G. P., "Variable Structure Control of Nonlinear Multivariable Systems: A Tutorial," *Proceedings of the IEEE*, Vol. 76, No. 3, 1988, pp. 212-232.

[12]DeCarlo, R., A., Zak, S. H., and Drakunov, S. V., "Section 57.5: Variable Structure, Sliding Mode Design," *The Control Handbook*, Levine, W. S. eds., CRC Press, Inc., Boca Raton, FL, 1996, pp. 941-951.

[13]Fernández, B. R., and Hedrick, J. K., "Control of Multivariable Non-Linear Systems by the Sliding Mode Method," *International Journal of Control*, Vol. 46, No. 3, 1987, pp. 1019-1040.

[14]Utkin, V. I., "Sliding Mode Control Design Principles and Applications to Electric Drives," *IEEE Transactions on Industrial Electronics*, Vol. 40, No. 1, 1993, pp. 23-36.

[15]Young, K. D., Utkin, V. I., and Özgüner, Ü., "A Control Engineer's Guide to Sliding Mode Control," *IEEE Transactions on Control Systems Technology*, Vol. 7, No. 3, 1999, pp. 328-342.

[16]Slotine, J.-J. E., and Li, W., *Applied Nonlinear Control*, Prentice Hall, Englewood Cliffs, NJ, 1991.

[17]Siwakosit, W., Snell, S. A., and Hess, R. A., "Robust Flight Control Design with Handling Qualities Constraints Using Scheduled Linear Dynamic Inversion and Loop-Shaping," *IEEE Transactions on Control Systems Technology*, Vol. 8, No. 3, 2000, pp. 483-494.

[18]Hess, R. A., "Unified Theory for Aircraft Handling Qualities and Adverse Aircraft-Pilot Coupling," *Journal of Guidance, Control, and Dynamics*, Vol. 20, No. 6, 1997, pp. 1141-1148.

[19]Maciejowski, J. M., "Chapt. 1," *Multivariable Feedback Design*, Addison-Wesley, Wokingham, UK, 1989,

[20]Hess, R. A., Zeyada, Y., and Heffley, R. K., "Modeling and Simulation for Helicopter Task Analysis," *Journal of American Helicopter Society*, submitted.

[21]Hess, R. A., Siwakosit, W., and Chung, J., "Accommodating a Class of Actuator Failures in Flight Control Systems," *Journal of Guidance, Control, and Dynamics*, Vol. 23, No. 3, 2000, pp. 412-419.

[22]Adams, R. J., Buffington, J. M., Sparks, A. G., and Banda, S. S., "An Introduction to Multivariable Flight Control Design," USAF Wright Laboratory, WL-TR-92-3110, Wright-Patterson AFB, OH, Oct, 1992.

[23]Shtessel, Y. B., Buffington, J. M., Pachter, M., Chandler, P.R., and Banda, S., S., "Reconfigurable Flight Control on Sliding Modes Addressing Actuator Deflections and Deflection Rate Saturation, AIAA Paper No. 98-4112.

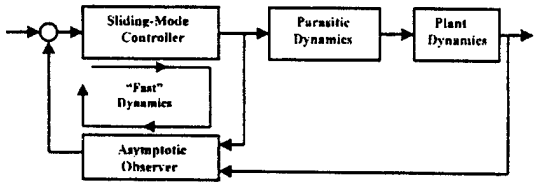

Figure 1 Asymptotic observers in SMC systems

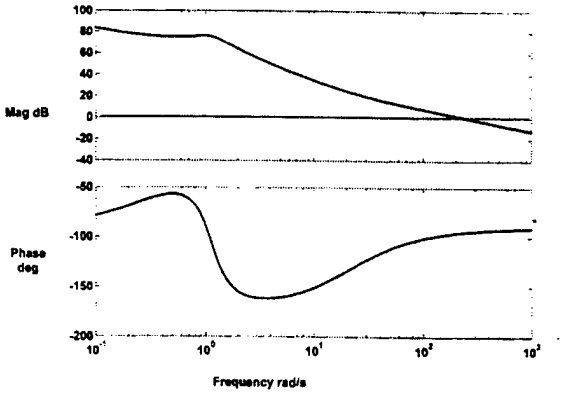

Figure 2 Loop transmission for SMC design, no actuators, flexible mode or observer included

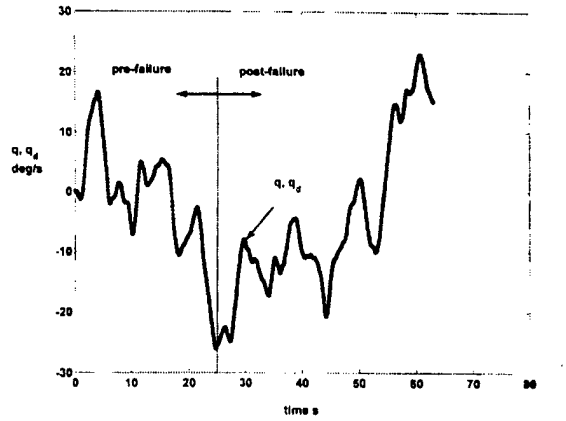

Figure 3 SMC tracking performance with sliding mode and failure. No actuator dynamics or observer included

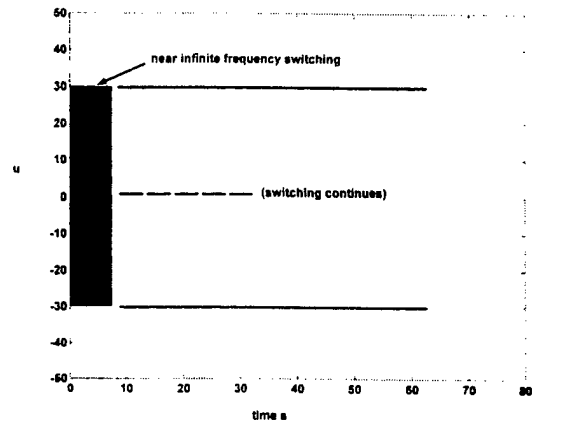

Figure 4 SMC pseudo-control input with sliding mode showing near-infinite frequency switching

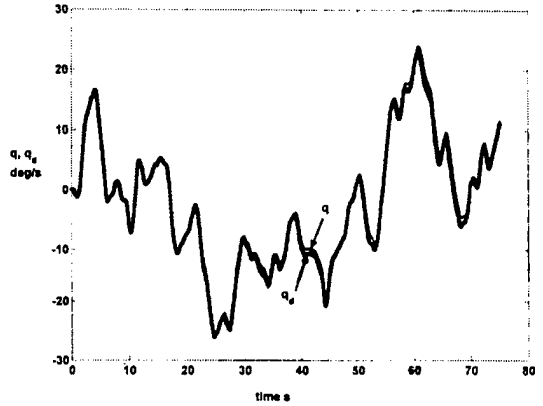

Figure 5 SMC tracking performance with boundary layer and failure. No actuator dynamics or observer included

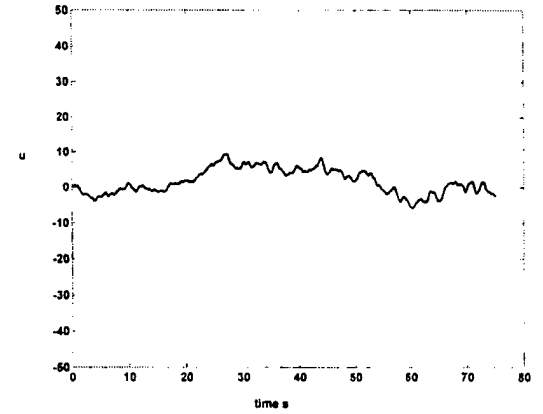

Figure 6 SMC pseudo-control input with boundary layer showing continuous control

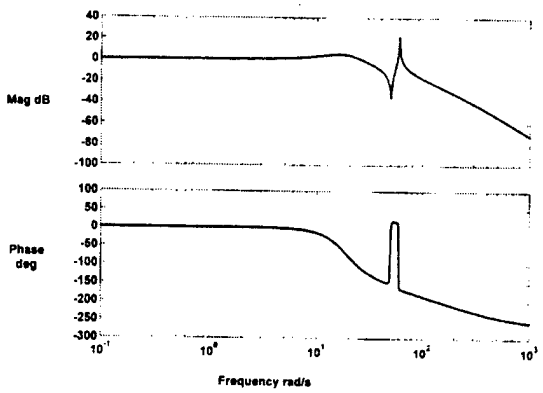

Figure 7 Closed loop SMC/vehicle transfer function from reference model output to vehicle pitch rate; actuators, flexible mode and observer included

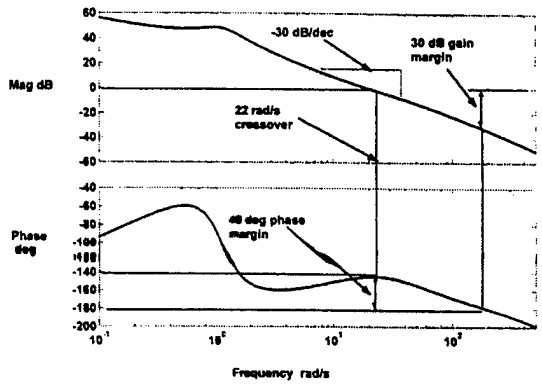

Figure 8 Effective unity feedback loop transmission for SMC design; flexible mode removed for clarity

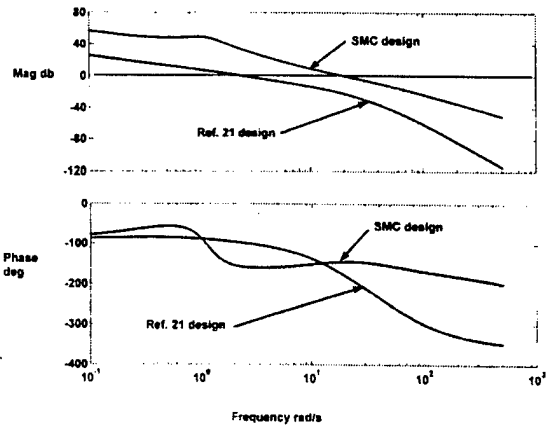

Figure 9 Comparison of loop transmission from SMC and Ref. 21 designs

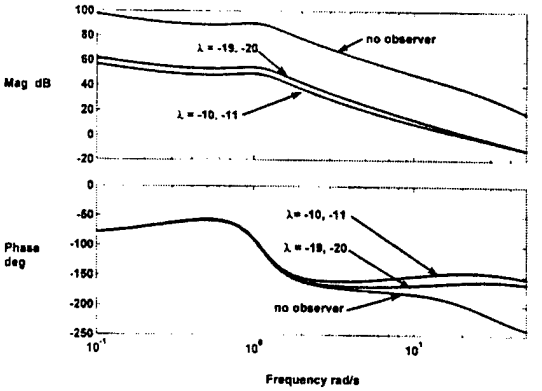

Figure 10 Loop transmission for SMC design without observer

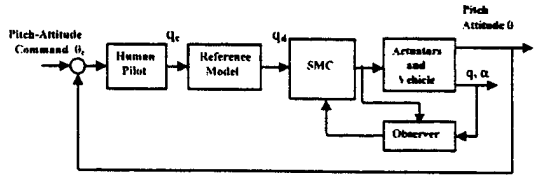

Figure 11 SMC system for pitch-attitude tracking

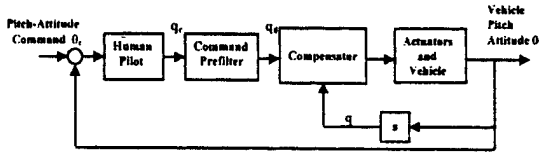

Figure 12 Ref. 21 system for pitch-attitude tracking

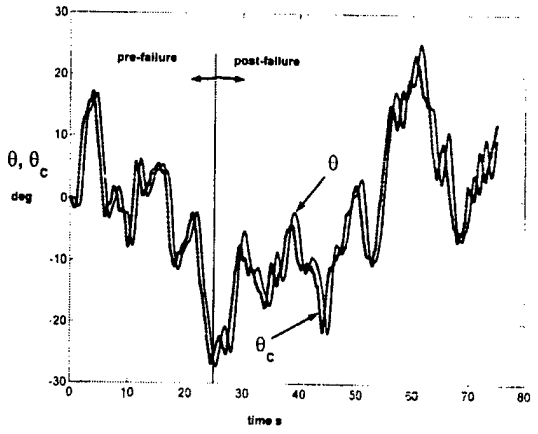

Figure 13 SMC pitch-attitude tracking before and after Failure No. 1

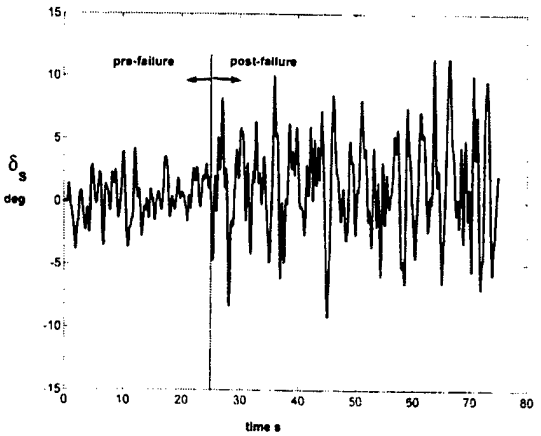

Figure 14 SMC stabilator time history before and after Failure No. 1

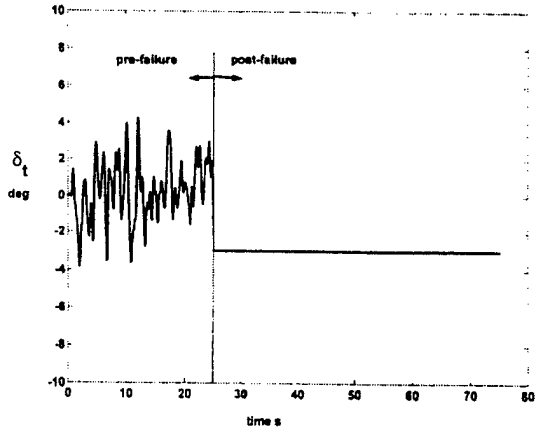

Figure 15 SMC thrust vector time history before and after Failure No. 1

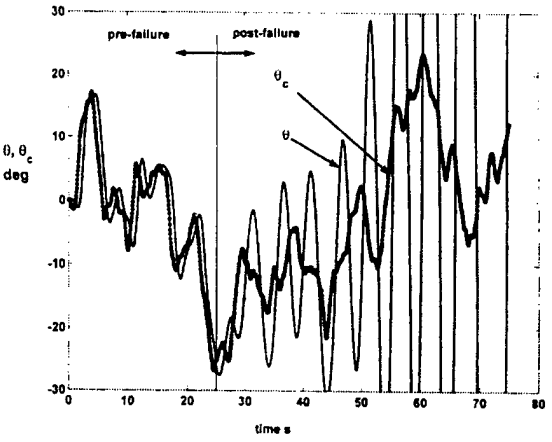

Figure 16 System of Fig. 12 (Ref. 21) pitch-attitude tracking before and after Failure No. 1

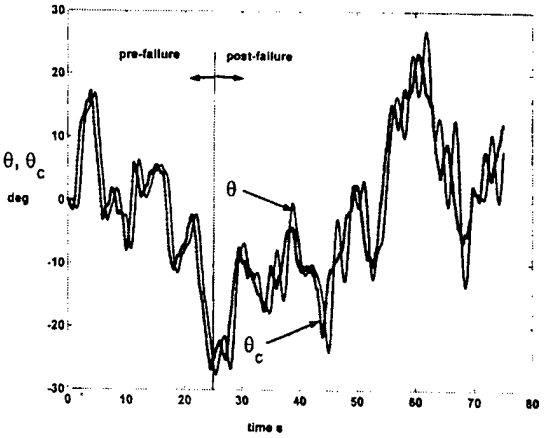

Figure 17 SMC pitch-attitude tracking before and after Failure No. 2

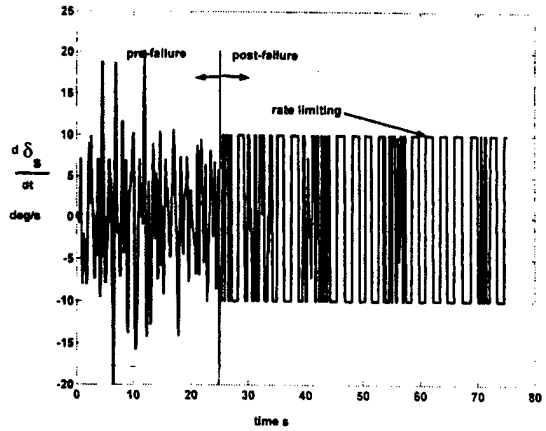

Figure 18 SMC stabilator-rate time history before and after Failure No. 2

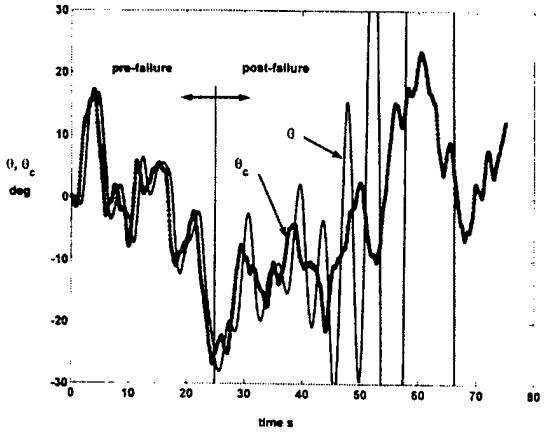

Figure 19 System of Fig. 12 (Ref. 21) pitch-attitude tracking before and after Failure No. 2

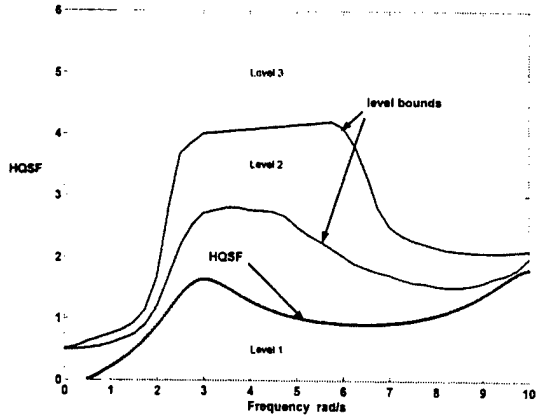

Figure 20 Handling qualities level prediction for SMC pitch-attitude tracking with Failure No. 1

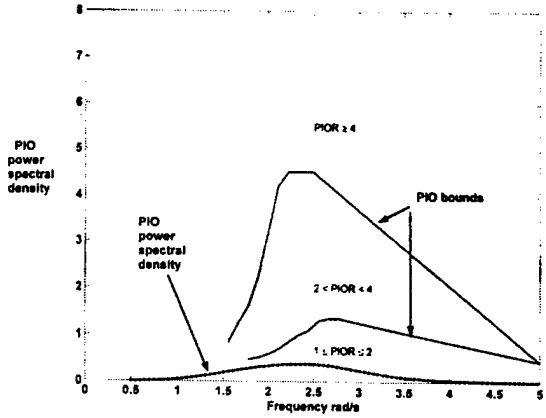

Figure 21 Pilot-induced oscillation (PIO) level prediction for SMC pitch-attitude tracking with Failure No. 1

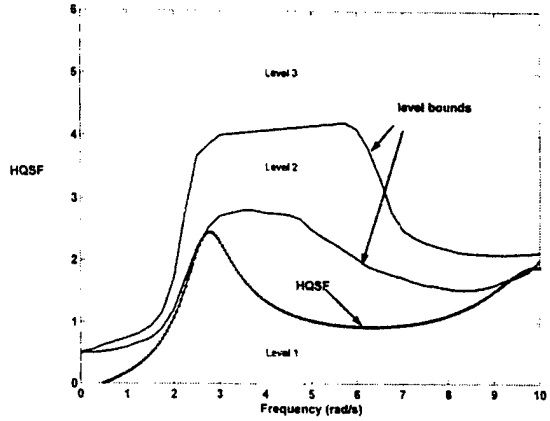

Figure 22 Handling qualities level prediction for SMC pitch-attitude tracking with Failure No. 2

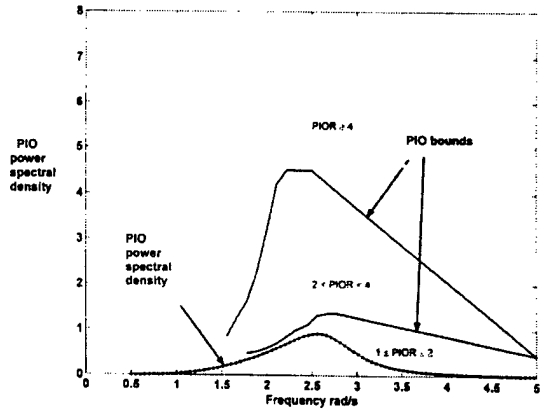

Figure 23 Pilot-induced oscillation (PIO) level prediction for SMC pitch-attitude tracking with Failure No. 1

MEMO FOR: AFIT/CIGS 30 Aug 2001

FROM: Maj Wells

SUBJECT: Submission of Clearance Request

1. Enclosed is a copy of a technical paper my advisor and I plan to present. Please review and clear for public release.

2. Per AFITI 36-105, Part 6.2.2.2 the following information is given:

   a. Name, Title and organization of authors
      i. Ronald A. Hess, Professor and Vice Chairman, Dept of Mechanical and Aero Engr, UC Davis, CA
      ii. Scott R. Wells, Maj, USAF, PhD Candidate, UC Davis
   b. Title of Presentation: Sliding Mode Control Applied to Reconfigurable Flight Control Design
   c. Where, when, how material is to be released:
      i. 40th AIAA Aerospace Sciences Meeting and Exhibit; Reno, NV
      ii. 14-17 Jan 2002
      iii. Oral presentation, with paper to be published in conference proceedings, paper number AIAA 2002-7751
      iv. Suspense Date for paper submittal: 1 Nov 01

3. This technical paper will probably be presented by Prof Hess. As coauthor, I have read and approved or have written all material associated with this paper and presentation. If Prof Hess so chooses, I may present the material myself.

4. Also enclosed is a completed Security and Policy Review Worksheet for AFIT/PA.

5. Upon approval, I can be reached at:

Scott Wells
1278 Antelope Ave
Davis, CA 95616
srwells@ucdavis.edu

Scott R. Wells, Maj, USAF